

# A global surface CO<sub>2</sub> flux dataset (2015–2022) inferred from OCO-2 retrievals using the GONGGA inversion system

Manuscript No. essd-2023-449

Zhe Jin, Xiangjun Tian, Yilong Wang, Hongqin Zhang, Min Zhao, Tao Wang, Jinzhi Ding, Shilong Piao

## Reply to reviewer 1

We would like to thank reviewer 1 for this thorough review and insightful comments, which significantly improved this manuscript. Please see below the point-to-point responses. All the line numbers indicated in this letter of response correspond to the revised version of text.

### Reviewer 1:

*This manuscript presents an 8-year dataset of surface-atmosphere CO<sub>2</sub> fluxes estimated by the GONGGA inversion system constrained by OCO-2 XCO<sub>2</sub> retrievals. This provides a useful dataset to the community and the paper is well written and structured to present the dataset and its evaluation. However, I feel that some important details are missing as described below. I recommend publication after addressing the following minor comments.*

**Response:** We thank the reviewer for the positive evaluation of our study and the valuable suggestions to improve it. We have carefully revised our manuscript following the comments and suggestions.

### Main comments:

1. *Sec. 2.1: Some details are missing here. What is the spatial and temporal resolution of the optimization. Is it at 2x2.5 and monthly (weekly)? How is the covariance between surface flux and atmospheric CO<sub>2</sub> constructed? If the set-up follows the set-up of a previous study that explicitly state this?*

### **Response:**

We optimized the surface flux at each grid cell of the transport model GEOS-Chem, where the size of each grid cell is 2°×2.5° (latitude×longitude). The temporal resolution of the optimization is 14 days, the same as the length of an inversion window.

GONGGA adopted a dual-pass inversion strategy, which first optimized the initial CO<sub>2</sub> concentrations in the CO<sub>2</sub> pass, and then optimized surface CO<sub>2</sub> fluxes in the flux pass (Jin et al., 2023). In the CO<sub>2</sub> pass, the prior error covariance was constructed through sampling from a historical CO<sub>2</sub> simulation. In the flux pass, the prior error covariance was constructed through the primary modes of historical fluxes, which would be introduced in more detail in the response to the second question. As these two

passes were performed successively, the prior errors from CO<sub>2</sub> concentrations and fluxes were assumed to be independent.

The link between surface flux and atmospheric CO<sub>2</sub> is constructed through the observation operator  $H(\cdot)$  which relies on GEOS-Chem simulations and sampling of modelled atmospheric CO<sub>2</sub>. Specifically, the atmospheric transport model is first used to simulate gridded CO<sub>2</sub> concentrations driven by surface fluxes. Then, the simulated gridded CO<sub>2</sub> profiles are interpolated horizontally by inverse distance weighting and vertically by linear interpolation on pressure. At last, the interpolated CO<sub>2</sub> profiles are used to construct the simulated XCO<sub>2</sub> with the equation:

$$XCO_2^m = XCO_2^a + \mathbf{h}^T \mathbf{A}(\mathbf{x}_{CO_2} - \mathbf{x}_{CO_2,a}).$$

where  $XCO_2^m$  is the modelled XCO<sub>2</sub>,  $XCO_2^a$  is the prior value provided by the OCO-2 Lite file,  $\mathbf{h}$  is the pressure weighting function,  $\mathbf{A}$  is the averaging kernel matrix,  $\mathbf{x}_{CO_2}$  is the interpolated CO<sub>2</sub> profile, and  $\mathbf{x}_{CO_2,a}$  is the prior CO<sub>2</sub> profile provided by the OCO-2 Lite file.

The set-up of GONGGA has been described in the previous study (Jin et al., 2023). In the revised manuscript, we added the description of the optimized fluxes and how they are connected with atmospheric CO<sub>2</sub> data:

- Line 122-124: “The spatial resolutions of the optimization for both initial CO<sub>2</sub> concentrations and fluxes are 2° latitude × 2.5° longitude, the same as the transport model resolution. The temporal resolution of the optimization is 14 days, indicating that the fluxes within each 14-day window are uniformly adjusted by the same scaling factor.”
- Line 107-115: “ $H(\cdot)$  is the observation operator, which relies on GEOS-Chem simulations and sampling of modelled atmospheric CO<sub>2</sub>. Firstly, the atmospheric transport model is used to simulate gridded CO<sub>2</sub> concentrations driven by surface fluxes. Then, the simulated gridded CO<sub>2</sub> profiles are interpolated horizontally by inverse distance weighting and vertically by linear interpolation on pressure. Thirdly, the interpolated CO<sub>2</sub> profiles are used to construct the simulated XCO<sub>2</sub> using the equation:

$$XCO_2^m = XCO_2^a + \mathbf{h}^T \mathbf{A}(\mathbf{x}_{CO_2} - \mathbf{x}_{CO_2,a}). \quad (2)$$

where  $XCO_2^m$  is the modelled XCO<sub>2</sub>,  $\mathbf{x}_{CO_2}$  is the interpolated CO<sub>2</sub> profile from the GEOS-Chem simulation.  $XCO_2^a$ ,  $\mathbf{h}$ ,  $\mathbf{A}$ , and  $\mathbf{x}_{CO_2,a}$  are the prior value of XCO<sub>2</sub>, the pressure weighting function, the averaging kernel matrix, and the prior CO<sub>2</sub> vertical profile, respectively, provided by the OCO-2 Lite file.”

2. *Sec. 2.2: How was prior error covariance matrix created? Is it diagonal? Is it an output of ORCHIDEE-MICT? Same question for ocean flux uncertainties. Based of Fig. 2 it seems that the global land and ocean uncertainties are very different in magnitude, despite the fact that the GCP gives similar order of magnitude uncertainties, why is this?*

**Response:**

The prior error covariance matrix was built using the ensemble perturbations (Text S1). It accounts for the spatial error covariances between fluxes at different grid cells

in the off-diagonal elements. Specifically, the prior perturbations of the scaling factors in the first inversion window were obtained through historical sampling. We first created a large ensemble of 108 samples of gridded monthly mean fluxes from January 2011 to December 2019, and divided them by the gridded fluxes of the first month of the inversion, with a value of 1 subsequently subtracted to form the ensemble of prior perturbations of scaling factors. Then we extracted 36 samples that could represent the primary modes of the big sample using Random State Variable (RSV) method (Zhang et al., 2020). Each sample comprises  $91 \times 144$  (latitude  $\times$  longitude) perturbation values, corresponding to one value per grid cell. The prior perturbations in the subsequent inversion windows were updated through the inversion following the method described in Tian et al. (2020). Both NEE and ocean-atmosphere fluxes applied this sample generation method. The historical NEE were from ORHIDEE-MICT simulations (Guimberteau et al., 2018), and historical ocean-atmosphere fluxes were from Takahashi climatology results (Takahashi et al., 2009). In the revised manuscript, we added the description on how the **B** matrix was built in Text S1:

- “The prior perturbations of the scaling factors in the first inversion window were obtained through historical sampling of fluxes. We first created 108 samples from historical fluxes, which consists of the monthly mean fluxes from January 1, 2011 to December 31, 2019. Then they divided the monthly mean flux in September 2014 and subtracted 1 to form the ensemble of perturbations of flux scaling factors. Subsequently, 36 samples that could represent the key spatial patterns of the large ensemble were extracted using Random State Variable (RSV) method (Zhang et al., 2020), forming the prior perturbations for the first inversion window. After the inversion of the first window, the prior perturbations of the next window were updated (Tian et al., 2020):

$$\mathbf{P}_x^{prior,w+1} = \mathbf{P}_x^{prior,w} \mathbf{V}_2 \Phi^T \quad (\text{S3})$$

Where  $\mathbf{P}_x^{prior,w+1}$  is the ensemble of the prior perturbations for the next window, and  $\mathbf{P}_x^{prior,w}$  is the ensemble of the prior perturbations for the current window. The matrix  $\mathbf{V}_2$  can be calculated by Eq. (S5-S7) detailed below, and  $\Phi^T$  is a random orthogonal matrix. The procedure was repeated through all inversion windows. Both NEE and ocean-atmosphere fluxes applied this sample generation method. The historical NEE were from ORHIDEE-MICT simulations (Guimberteau et al., 2018), and historical ocean-atmosphere fluxes were from Takahashi climatology results (Takahashi et al., 2009). As a result, the total uncertainty of our prior land and ocean fluxes at a global scale and for a full year, before assimilating XCO<sub>2</sub> observations, amount to an average of 4.7 Pg C yr<sup>-1</sup> and 0.28 Pg C yr<sup>-1</sup>, respectively.”

Figure 2 shows the posterior uncertainty of land and ocean fluxes, which are the estimates from the Bayesian statistics. They are different from the large spread of the ensemble of process-based models or inversion models in GCP, which encompasses many more sources of uncertainties. The variations among process-based models come from different processes included, different equations to describe the key processes, and their parameterizations. The inversion models can vary in the atmospheric transport

models, the inversion algorithm, the prior fluxes, and assimilated observations. We think it is difficult to directly compare the Bayesian statistic posterior uncertainty with the spread of GCP model ensemble. In GONGGA, the total annual uncertainty of our prior land and ocean fluxes on a global scale, before assimilating XCO<sub>2</sub> observations, amount to 4.7 Pg C yr<sup>-1</sup> and 0.28 Pg C yr<sup>-1</sup>, which is on the same order of magnitude as other inversion systems. For instance, the 1- $\sigma$  uncertainty for the prior land and air-sea fluxes in the CAMS inversion system (Chevallier, 2021) are 3.0 Pg C yr<sup>-1</sup> and 0.5 Pg C yr<sup>-1</sup>, respectively.

For the posterior uncertainty shown in Fig. 2, we found a code mistake in our calculation, which did not account for the error coherence in time within an inversion window as the 14 days share the same scaling factor. After the correction, the average posterior uncertainty of land and ocean fluxes are 4.3 Pg C yr<sup>-1</sup> and 0.25 Pg C yr<sup>-1</sup>, respectively. We updated the posterior uncertainty in Fig. 2 in the revised manuscript, which is also shown here as Fig. R1.

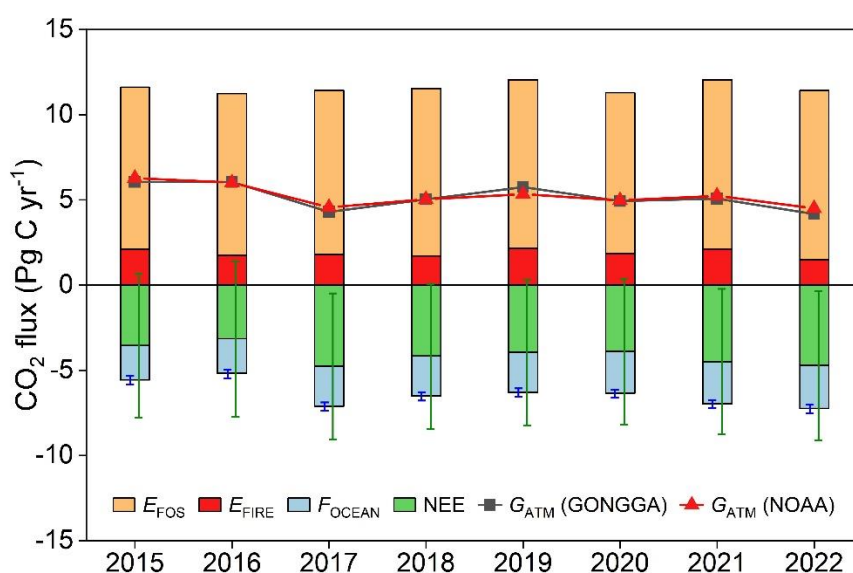


**Figure R1. Global carbon budget estimated by GONGGA and atmospheric CO<sub>2</sub> growth rate from NOAA during 2015–2022.**

3. Sec 2.3. The OCO-2 XCO<sub>2</sub> dataset is not properly cited. There is the v11r standard XCO<sub>2</sub> product (no bias correction, JPL DEM, still running routinely), the v11r Lite XCO<sub>2</sub> product (bias corrected, JPL NASADEM+, available up to April 2023) and the v11.1r Lite XCO<sub>2</sub> product (bias corrected, Copernicus DEM, still running routinely). Please clearly state and cite which dataset was used. An important point is that the DEM used in v11r cause a systematic error over the northern high latitudes that may have impacted the inversion results, if used. The impact of the DEM change is described in Jacobs et al. (2023): <https://doi.org/10.5194/amt-2023-151>. Instructions for citing the OCO-2 retrievals are given on the GES DISC website. For example, if this was V11.1r downloaded from GES DISC then citation should be: OCO-2/OCO-3 Science Team, Vivienne Payne, Abhishek Chatterjee (2022), OCO-2 Level 2 bias-corrected

*XCO<sub>2</sub> and other select fields from the full-physics retrieval aggregated as daily files, Retrospective processing V11.1r, Greenbelt, MD, USA, Goddard Earth Sciences Data and Information Services Center (GES DISC), Accessed: [Data Access Date], 10.5067/8E4VLCK16O6Q”*

**Response:**

We used the v11r Lite XCO<sub>2</sub> product in this submission. We thank the reviewer for directing us to the recent paper on the potential biases in v11r XCO<sub>2</sub> retrievals in the northern high latitudes. We are now starting to run the inversion with the latest v11.1r product. The preliminary results from 2015 to 2018 show that the inverted land carbon sinks north of 60°N using v11.1r are smaller than those using v11r by 90 to 140 Tg C yr<sup>-1</sup>, and accompanied by a compensating increase in ocean carbon uptake in the northern mid- and low- latitudinal band (Fig. R2).

In the revised manuscript, we added the reference for the data version and a paragraph to discuss the uncertainty related to the different versions of OCO-2 retrieval products:

- Line 417-427: “In the current version of GONGGA, we assimilated the OCO-2 v11r Lite XCO<sub>2</sub> dataset. A recent paper found that the v11r Lite product has a bias of -0.4 to -0.8 ppm across regions north of 60°N due to the variations of digital elevation model (DEM) used in the retrieval algorithm (Jacobs et al., 2024), and this bias introduces a ~ 100 Tg C shift in the partitioning of carbon fluxes for the latitudinal bands. A preliminary test of GONGGA using the latest v11.1r Lite product showed the inverted terrestrial carbon sink tends to be 90 to 140 Tg C yr<sup>-1</sup> lower north of 60° N than using the v11r Lite product, consistent with the previous findings. In addition, some parts of GONGGA’s inversion algorithm, such as the data selection, were partly different from those proposed by the OCO-2 Science Team (Peiro et al., 2022; Byrne et al., 2023; Baker et al., 2022), but GONGGA’s inversion results were broadly consistent with the ensemble of OCO-2 MIP inversions and GCB2023, and gave reasonable estimates of global and regional carbon budgets within the uncertainties. In the future, GONGGA will regularly publish new versions of inverted fluxes using the latest OCO-2 data on an annual basis. These updates will align with the latest suggestions from the OCO-2 Science Team, enabling the ongoing monitoring of CO<sub>2</sub> fluxes.”

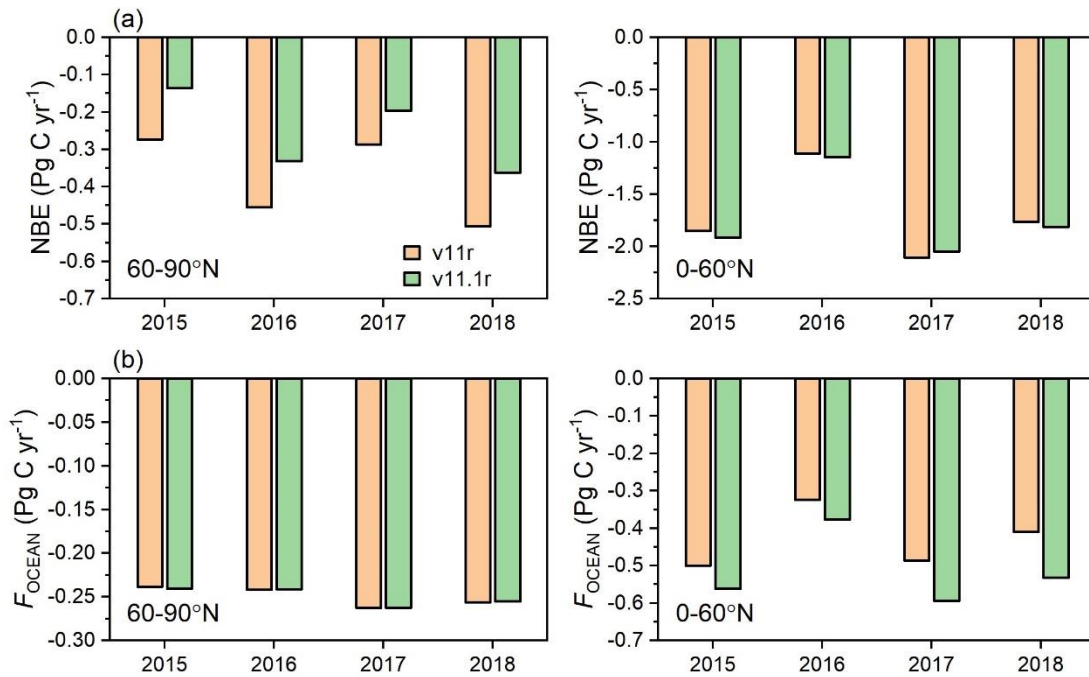


**Figure R2.** The inverted (a) NBE and (b)  $F_{\text{OCEAN}}$  in regions north of 60°N and 0-60°N from GONGGA inversions using OCO-2 v11r retrievals (orange bars) and v11.1r (green bars) retrievals during 2015-2018.

4. L190-191: I think that the definition “ $S_{\text{LAND}}$ ” is confusing here. In the Global Carbon Budget papers, the term  $S_{\text{LAND}}$  is the net land sink after accounting for net land-use change emissions. However, in this paper,  $S_{\text{LAND}}$  is defined as NEE (e.g.,  $S_{\text{LAND}} = \text{NEE} - \text{Fire}$ ). But fire does not equal  $E_{\text{LUC}}$ , so the definitions are different. I recommend not using  $S_{\text{LAND}}$  to define this quantity. It may be best to compare the NBE terms between the two studies after accounting for lateral fluxes. I recommend reviewing Sec. 7 of Byrne et al. (2023; <https://essd.copernicus.org/articles/15/963/2023/>) to see a comparison between the OCO-2 v10 MIP and Global Carbon Budget numbers.

**Response:**

Thank you for clarifying the differences between the two flux terms. To avoid confusion, we changed the notation and reported NEE for the terrestrial atmosphere-surface CO<sub>2</sub> exchange except biomass burning emissions, which is the value directly estimated by the inversion. In addition, when comparing our inversion results with GCB estimates in the last paragraph of Section 4.1, we adjusted GONGGA’s NBE estimates to account for the lateral flux of carbon transported by rivers as reported by GCB. Note that we also changed GCB values to the latest estimates (GCB2023) in the revised manuscript. The manuscript was revised as follows:

- Line 203-205: “Here, we present the five major components of the global carbon budget, including the fossil fuel CO<sub>2</sub> emissions ( $E_{\text{FOS}}$ ), biomass burning emissions ( $E_{\text{FIRE}}$ ), atmospheric CO<sub>2</sub> concentration growth rate ( $G_{\text{ATM}}$ ), ocean CO<sub>2</sub> flux ( $F_{\text{OCEAN}}$ ), and NEE (Fig. 2).”

- Line 219-232: “We also compared net biosphere exchange (NBE, i.e., the net carbon flux of all the land-atmosphere exchange processes except fossil fuel emissions, calculated as  $NEE + E_{\text{FIRE}}$ ) and ocean sink estimated from the GONGGA inversion with GCB2023. Note that the GCB2023 estimations represent the carbon accumulated in the land and ocean reservoirs. We followed GCB2023’s definitions and adjusted riverine  $\text{CO}_2$  transport from the net atmosphere-surface  $\text{CO}_2$  exchange over land (NBE) and ocean ( $F_{\text{OCEAN}}$ ). Specifically, pre-industrial lateral carbon transport through the land-ocean aquatic continuum (LOAC) of  $0.65 \pm 0.35 \text{ Pg C yr}^{-1}$  (Regnier et al. (2022)) was subtracted from  $-NBE$  to represent land carbon sink, and added to  $-F_{\text{OCEAN}}$  to represent ocean carbon sink. During 2015-2022, the mean of corrected land carbon sink from GONGGA was  $1.57 \pm 0.67 \text{ Pg C yr}^{-1}$ , and the mean of corrected ocean sink was  $2.97 \pm 0.18 \text{ Pg C yr}^{-1}$ . GCB2023’s estimate of ocean sink was  $2.88 \pm 0.07 \text{ Pg C yr}^{-1}$  based on global ocean biogeochemistry models and surface ocean  $f\text{CO}_2$ -observation-based products. The land carbon sink from GCB2023 was  $2.00 \pm 0.62 \text{ Pg C yr}^{-1}$  from the dynamic global vegetation models (DGVMs) and was  $1.55 \pm 0.77 \text{ Pg C yr}^{-1}$  calculated as the residual sink from the global budget of fossil fuel emissions, atmospheric growth rate and ocean sink (Friedlingstein et al., 2023). As the estimate of land carbon sink from DGVMs will introduce a budget imbalance in GCB2023, our estimates are well consistent with GCB2023’s estimates based on ocean models and the residual land sink and close the global budget.”

Specific comments:

1. L25: *Specify that these are in situ and flask  $\text{CO}_2$  ObsPack data.*

**Response:**

We revised the sentence to “The dataset was evaluated by comparing posterior  $\text{CO}_2$  simulations with Total Carbon Column Observing Network (TCCON) retrievals as well as Observation Package (ObsPack) surface flask observations and aircraft observations.” in Line 23-25.

2. L102-103: *I think Liu et al. (2021) optimized NBE, so may not be an applicable reference.*

**Response:**

We revised the references to include only those inversions that optimize NEE.

3. L115: *“to December 21, 2022”. Typically, inversions have a spin down period to increase data constraints at the end of the period, why was the inversion not extended into 2023?*

**Response:**

GONGGA adopts the approach to optimize fluxes within each inversion window of 14 days. Once the fluxes were already optimized in previous windows, they will not change when the inversion window moves on. So we think that even a spin-down period

of the inversion till 2023 will not change our results for 2015-2022. Most studies using such an approach with limited length of inversion window usually do not include a spin down period (Jiang et al., 2022; Peters et al., 2007; Kong et al., 2022).

We agree with the reviewer that some inversions assimilating *in-situ* observations with the 4DVar algorithm and optimizing the full-time series of fluxes include a spin down period to account for the fact that the signal from a flux emitted in the Northern Hemisphere may take about 1 year to reach the Southern Hemisphere. However, we think that this issue may be of less concern when assimilating satellite XCO<sub>2</sub> observations compared to assimilating surface *in-situ* observations, given the fact that the wide coverage of satellite retrievals can capture the inter-hemisphere transport more easily and attribute the fluxes to its sources.

In addition, we show the time series of biases in the modelled CO<sub>2</sub> driven by posterior fluxes against the TCCON and ObsPack data in Fig. R3 and Fig. R4. At most stations, the biases in the year 2022 were similar to previous years and no significant trends were found, confirming that our estimates of fluxes in 2022 were not biased.

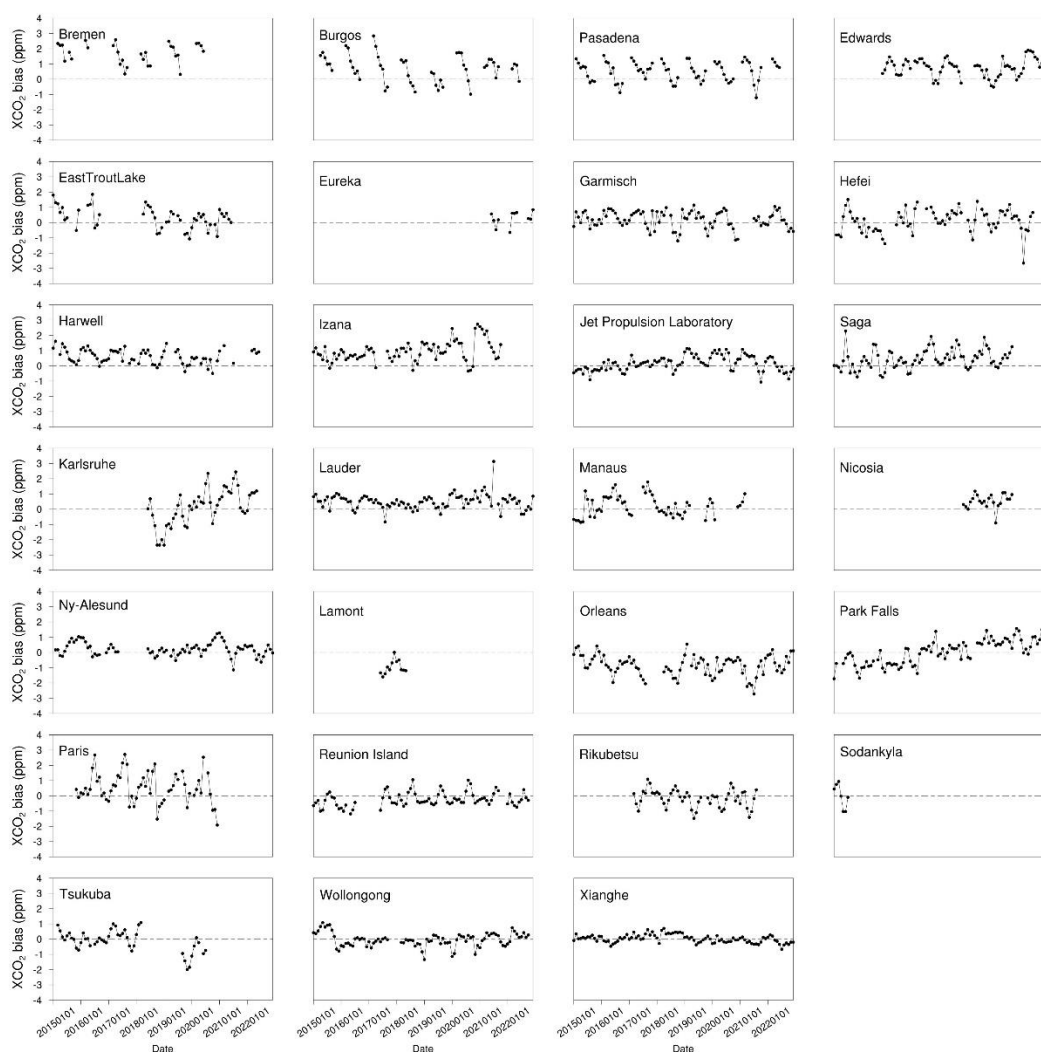


**Figure R3. Time series of monthly bias between TCCON retrievals and posterior simulations at each TCCON site (posterior simulation - retrieval).**



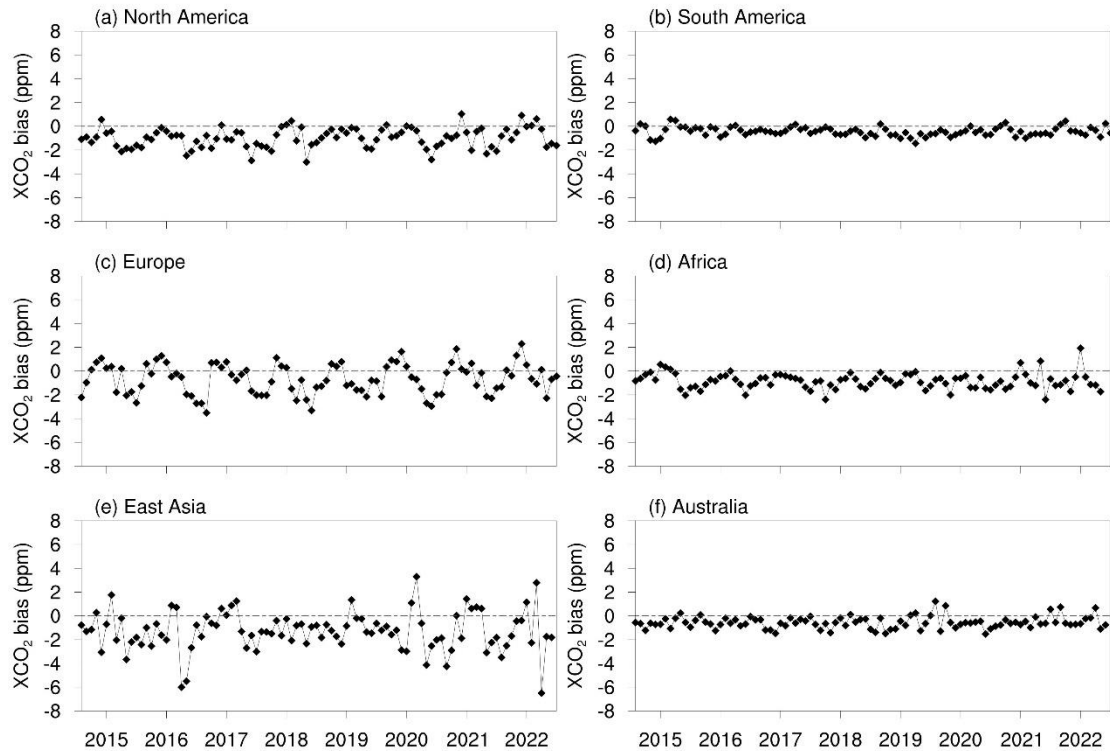


**Figure 4. Time series of monthly bias between ObsPack surface flask observations and posterior simulations for the six sub-regions (posterior simulation - observation).**

4. Table 1 should be referenced in Sec. 2.4.1

**Response:**

We moved Table 1 to Sec. 2.4.1 and added the reference in the revised text as you recommended.

5. L183: would be clearer to say “ocean-atmosphere” than “ocean”

**Response:**

Thank you for the suggestion to make the text clearer. We changed the “ocean flux” to “ocean-atmosphere flux” throughout the manuscript following your recommendation.

6. L193-194: “NEE had substantial interannual variability ( $-4.08 \pm 0.53 \text{ PgC yr}^{-1}$ )”. This phrasing makes it seem like  $-4.08$  is the interannual variability. I would suggest re-phrasing “NEE had substantial mean sink with considerable interannual variability, estimated as the standard deviation across years ( $-4.08 \pm 0.53 \text{ PgC yr}^{-1}$ )”.

**Response:**

Thank you for the suggestion. We revised this sentence to “Over these 8 years, NEE exhibited a substantial mean sink with considerable interannual variability, estimated

as the standard deviation across years ( $-4.08 \pm 0.53 \text{ Pg C yr}^{-1}$ .)” in Line 207-208.

7. L232: *These are the incorrect citations for the v10 OCO-2 MIP. The documentation of the OCO-2 v10 MIP should be cited as:*

*Byrne, B., Baker, D. F., Basu, S., Bertolacci, M., Bowman, K. W., Carroll, D., Chatterjee, A., Chevallier, F., Ciais, P., Cressie, N., Crisp, D., Crowell, S., Deng, F., Deng, Z., Deutscher, N. M., Dubey, M. K., Feng, S., García, O. E., Griffith, D. W. T., Herkommer, B., Hu, L., Jacobson, A. R., Janardanan, R., Jeong, S., Johnson, M. S., Jones, D. B. A., Kivi, R., Liu, J., Liu, Z., Maksyutov, S., Miller, J. B., Miller, S. M., Morino, I., Notholt, J., Oda, T., O'Dell, C. W., Oh, Y.-S., Ohyama, H., Patra, P. K., Peiro, H., Petri, C., Philip, S., Pollard, D. F., Poulter, B., Remaud, M., Schuh, A., Sha, M. K., Shiomi, K., Strong, K., Sweeney, C., Té, Y., Tian, H., Velazco, V. A., Vrekoussis, M., Warneke, T., Worden, J. R., Wunch, D., Yao, Y., Yun, J., Zammit-Mangion, A., and Zeng, N.: National CO<sub>2</sub> budgets (2015–2020) inferred from atmospheric CO<sub>2</sub> observations in support of the global stocktake, *Earth Syst. Sci. Data*, 15, 963–1004, <https://doi.org/10.5194/essd-15-963-2023>, 2023.*

*While the dataset should be cited as:*

*Baker, D. F., Basu, S., Bertolacci, M., Chevallier, F., Cressie, N., Crowell, S., Deng, F., He, W., Jacobson, A. R., Janardanan, R., Jiang, F., Johnson, M. S., Jones, D. B. A., Liu, J., Liu, Z., Maksyutov, S., Miller, S. M., Philip, S., Schuh, A., Weir, B., Zammit-Mangion, A., and Zeng, N.: v10 Orbiting Carbon Observatory-2 model intercomparison project, NOAA Global Monitoring Laboratory [data set], [https://gml.noaa.gov/ccgg/OCO2\\_v10mip/](https://gml.noaa.gov/ccgg/OCO2_v10mip/), last access: . XXX*

**Response:**

Thank you for pointing this out, we corrected the citations for the v10 OCO-2 MIP.

8. L245-248: *It could be interesting to plot the GONGGA prior and OCO v10 MIP priors as a supplementary figure. Would be interesting if these differences are also present there.*

**Response:**

Thank you for your suggestion. We replaced Fig. S1 with the prior estimates from GONGGA and OCO-2 MIP, considering that the posterior GONGGA estimates were presented in Fig. 5. We also put it here as Fig. R5. It is shown that Boreal North America was a carbon source in GONGGA's prior, while it was a carbon sink in OCO-2 MIP prior. The inverted fluxes from GONGGA and OCO-2 MIP were both carbon sinks, but the size of the sink in GONGGA was smaller than OCO-2 MIP. It is similar for Northern Africa where GONGGA and OCO-2 MIP prior both estimated it as a carbon sink, while the inverted fluxes from GONGGA and OCO-2 MIP were both carbon sources. The larger carbon source from OCO-2 MIP aligned with the smaller prior carbon sink than GONGGA. The manuscript was revised as follows:

- Line 260-270: “GONGGA showed good agreement with OCO-2 MIP inversions for most regions, and divergences occurred mainly in Boreal North America and

Northern Africa. The difference between GONGGA and OCO-2 MIP inversions may be related to the prior NBE adopted and retrieval pre-processing methods utilized. In Boreal North America, GONGGA’s prior emerged as a carbon source, whereas OCO-2 MIP’s prior was a carbon sink (Fig. S1). After assimilating OCO-2 retrievals, GONGGA and OCO-2 MIP consistently showed Boreal North America was a carbon sink, but the sink in GONGGA was smaller than OCO-2 MIP. The same situation happened in Northern Africa. Both GONGGA’s prior and OCO-2 MIP’s prior estimated Northern Africa as a terrestrial carbon sink, but the sink from GONGGA was stronger than that from OCO-2 MIP (Fig. S1). Constrained by OCO-2 retrievals, both GONGGA and OCO-2 MIP estimated it as a carbon source, and the source from GONGGA was weaker than that from OCO-2 MIP, aligning with the sizes of their prior sinks. In addition, the impact of prior fluxes may be amplified by the insufficient coverage of OCO-2 retrievals.”

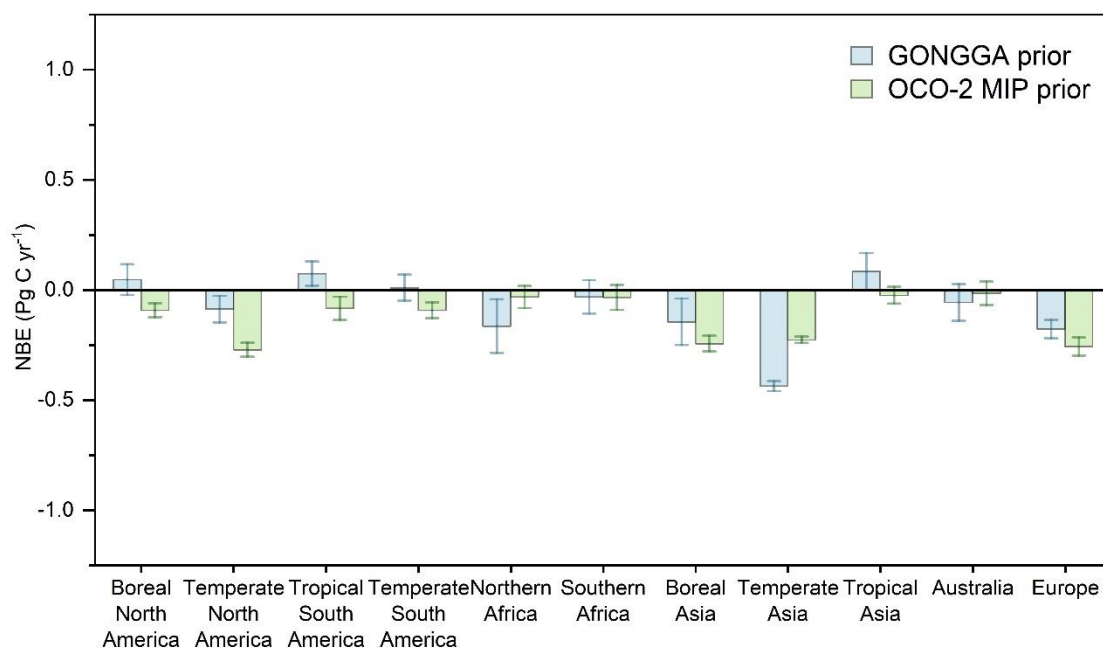


**Figure R5. Annual mean (2015–2022) NBE at 11 TransCom land regions from GONGGA prior and OCO-2 MIP prior estimates. The error bar of NBE represents the multi-year standard deviation.**

9. L258-259: I don’t understand the logic in this sentence: “In the Amazon, the mean gross emissions from forest fires from 2003 to 2015 was  $454 \pm 496 \text{ Tg CO}_2 \text{ yr}^{-1}$ , which may counteract the decline of Amazon deforestation carbon emissions (Aragão et al., 2018).”

**Response:**

To make things clearer, we moved this paragraph to the discussion section and rewrote this sentence as: “In the Amazon, despite the decline of deforestation rate during 2003-2015, carbon emissions from drought-induced fires had increased very quickly (Aragão et al., 2018).” in Line 398-400.

10. L260: *In addition to van der Velde et al. (2021), there were two studies that examined the CO<sub>2</sub> emissions from the 2019-20 Australian fires using OCO-2 data:*

1. Byrne, B., Liu, J., Lee, M., Yin, Y., Bowman, K. W., Miyazaki, K., et al. (2021). *The carbon cycle of southeast Australia during 2019–2020: Drought, fires, and subsequent recovery.* *AGU Advances*, 2, e2021AV000469. <https://doi.org/10.1029/2021AV000469>

2. Wang, J., Liu, Z., Zeng, N., Jiang, F., Wang, H., & Ju, W. (2020). *Spaceborne detection of XCO<sub>2</sub> enhancement induced by Australian mega-bush-fires.* *Environmental Research Letters*, 15(12), 124069. <https://doi.org/10.1088/1748-9326/abc846>

**Response:**

Thank you for mentioning these references. We added them in the text as recommended.

11. L272: *Please be more specific. I suggest re-writing “the magnitude of global NBE IAV” as “the standard deviation of global NBE IAV”.*

**Response:**

Indeed, we calculated the NBE IAV as the standard deviation of NBE across years. To be clearer, we revised this sentence to “We computed the standard deviation of global NBE to represent its magnitude of IAV, which amounted to 0.63 Pg C yr<sup>-1</sup> during the 2015–2022 period.” in Line 282-284.

12. L276-277: *“Considering the short time series of the carbon cycle, the latitudinal contributions in this study are qualitative, rather than quantitative.” I think this would be better written as “Considering the short time series of the carbon cycle, the latitudinal contributions in this study are suggestive but not statistically robust.”*

**Response:**

We revised this sentence to “Given the short time series of the inversion, the latitudinal contributions in this study are suggestive but not statistically conclusive.” in Line 288-289.

13. L298: *“more flatten” should be “smaller amplitude”*

**Response:**

Thank you for the suggestion. We revised the sentence to “In the tropics, however, the seasonal cycles have smaller amplitudes and the shapes are distinct in different years.” in Line 308.

14. *Figure 9-12 captions. Specify “posterior simulations”*

**Response:**

We added “posterior simulations” in Figure 9-12 captions and explained in the text that it means “the simulation is driven by posterior fluxes” in Line 333.

15. L363: *Just for your information, there is a known difference in the mean atmospheric CO<sub>2</sub> abundance between TCCON and posterior CO<sub>2</sub> fields from in situ inversions, which is not well understood. I'm not sure if this has been documented in a paper; but it is known to some researchers. This could cause the differences seen here.*

**Response:**

Thank you for the information. We found in Polavarapu et al., (2018) and Peiro et al., (2022) that the posterior CO<sub>2</sub> simulations from *in-situ* inversions exhibited high positive biases relative to TCCON retrievals in northern mid- to high- latitudes. We will keep on following the latest studies.

16. Q: L366: *BIAS shouldn't be all capitalized.*

**Response:**

Thank you for the suggestion. We changed all “BIAS” to “bias”.

## References

- Aragão, L. E. O. C., Anderson, L. O., Fonseca, M. G., Rosan, T. M., Vedovato, L. B., Wagner, F. H., Silva, C. V. J., Silva Junior, C. H. L., Arai, E., Aguiar, A. P., Barlow, J., Berenguer, E., Deeter, M. N., Domingues, L. G., Gatti, L., Gloor, M., Malhi, Y., Marengo, J. A., Miller, J. B., Phillips, O. L., and Saatchi, S.: 21st Century drought-related fires counteract the decline of Amazon deforestation carbon emissions, *Nature Communications*, 9, 536, <https://doi.org/10.1038/s41467-017-02771-y>, 2018.
- Baker, D. F., Bell, E., Davis, K. J., Campbell, J. F., Lin, B., and Dobler, J.: A new exponentially decaying error correlation model for assimilating OCO-2 column-average CO<sub>2</sub> data using a length scale computed from airborne lidar measurements, *Geosci. Model Dev.*, 15, 649-668, 10.5194/gmd-15-649-2022, 2022.
- Byrne, B., Baker, D. F., Basu, S., Bertolacci, M., Bowman, K. W., Carroll, D., Chatterjee, A., Chevallier, F., Ciais, P., Cressie, N., Crisp, D., Crowell, S., Deng, F., Deng, Z., Deutscher, N. M., Dubey, M. K., Feng, S., García, O. E., Griffith, D. W. T., Herkommer, B., Hu, L., Jacobson, A. R., Janardanan, R., Jeong, S., Johnson, M. S., Jones, D. B. A., Kivi, R., Liu, J., Liu, Z., Maksyutov, S., Miller, J. B., Miller, S. M., Morino, I., Notholt, J., Oda, T., O'Dell, C. W., Oh, Y. S., Ohyama, H., Patra, P. K., Peiro, H., Petri, C., Philip, S., Pollard, D. F., Poulter, B., Remaud, M., Schuh, A., Sha, M. K., Shiomi, K., Strong, K., Sweeney, C., Té, Y., Tian, H., Velasco, V. A., Vrekoussis, M., Warneke, T., Worden, J. R., Wunch, D., Yao, Y., Yun, J., Zammit-Mangion, A., and Zeng, N.: National CO<sub>2</sub> budgets (2015–2020) inferred from atmospheric CO<sub>2</sub> observations in support of the global stocktake, *Earth Syst. Sci. Data*, 15, 963-1004, 10.5194/essd-15-963-2023, 2023.
- Chevallier, F.: Validation report for the CO<sub>2</sub> fluxes estimated by atmospheric inversion, v20r2 Version 1.0, 2021.
- Friedlingstein, P., O'Sullivan, M., Jones, M. W., Andrew, R. M., Bakker, D. C. E., Hauck, J., Landschützer, P., Le Quéré, C., Luijkx, I. T., Peters, G. P., Peters, W., Pongratz, J., Schwingshackl, C., Sitch, S., Canadell, J. G., Ciais, P., Jackson, R. B., Alin, S. R., Anthoni, P., Barbero, L., Bates, N. R., Becker, M., Bellouin, N., Decharme, B., Bopp, L., Brasika, I. B. M., Cadule, P., Chamberlain, M. A., Chandra, N., Chau, T. T. T., Chevallier, F., Chini, L. P., Cronin, M., Dou, X., Enyo, K., Evans, W., Falk, S., Feely, R. A., Feng, L., Ford, D. J., Gasser, T., Ghattas, J., Gkritzalis, T., Grassi, G., Gregor, L., Gruber, N., Gürses, Ö., Harris, I., Hefner, M., Heinke, J., Houghton, R. A., Hurtt, G. C., Iida, Y., Ilyina, T., Jacobson, A. R., Jain, A., Jarníková, T., Jersild, A., Jiang, F., Jin, Z., Joos, F., Kato, E., Keeling, R. F., Kennedy, D., Klein Goldewijk, K., Knauer, J., Korsbakken, J. I., Körtzinger, A., Lan, X., Lefèvre, N., Li, H., Liu, J., Liu, Z., Ma, L., Marland, G., Mayot, N., McGuire, P. C., McKinley, G. A., Meyer, G., Morgan, E. J., Munro, D. R., Nakaoka, S. I., Niwa, Y., O'Brien, K. M., Olsen, A., Omar, A. M., Ono, T., Paulsen, M., Pierrot, D., Pockock, K., Poulter, B., Powis, C. M., Rehder, G., Resplandy, L., Robertson, E., Rödenbeck, C., Rosan, T. M., Schwinger, J., Séférian, R., Smallman, T. L., Smith, S. M., Sospedra-Alfonso, R., Sun, Q., Sutton, A. J., Sweeney, C., Takao, S., Tans, P. P., Tian, H., Tilbrook, B., Tsujino, H., Tubiello, F., van der Werf, G. R., van Ooijen, E., Wanninkhof, R., Watanabe, M., Wimart-Rousseau, C., Yang, D., Yang, X., Yuan, W., Yue, X., Zaehle, S., Zeng, J., and Zheng, B.: Global Carbon Budget 2023, *Earth Syst. Sci. Data*, 15, 5301-5369, 10.5194/essd-15-5301-2023, 2023.
- Guimberteau, M., Zhu, D., Maignan, F., Huang, Y., Yue, C., Dantec-Nédélec, S., Otlé, C., Jornet-Puig, A., Bastos, A., Laurent, P., Goll, D., Bowring, S., Chang, J., Guenet, B., Tifafi, M., Peng, S., Krinner, G., Ducharne, A., Wang, F., Wang, T., Wang, X., Wang, Y., Yin, Z., Lauerwald, R., Joetzer, E., Qiu,

- C., Kim, H., and Ciais, P.: ORCHIDEE-MICT (v8.4.1), a land surface model for the high latitudes: model description and validation, *Geosci. Model Dev.*, 11, 121-163, 10.5194/gmd-11-121-2018, 2018.
- Jacobs, N., O'Dell, C. W., Taylor, T. E., Logan, T. L., Byrne, B., Kiel, M., Kivi, R., Heikkinen, P., Merrelli, A., Payne, V. H., and Chatterjee, A.: The importance of digital elevation model accuracy in XCO<sub>2</sub> retrievals: improving the Orbiting Carbon Observatory 2 Atmospheric Carbon Observations from Space version 11 retrieval product, *Atmos. Meas. Tech.*, 17, 1375-1401, 10.5194/amt-17-1375-2024, 2024.
- Jiang, F., Ju, W., He, W., Wu, M., Wang, H., Wang, J., Jia, M., Feng, S., Zhang, L., and Chen, J. M.: A 10-year global monthly averaged terrestrial net ecosystem exchange dataset inferred from the ACOS GOSAT v9 XCO<sub>2</sub> retrievals (GCAS2021), *Earth System Science Data*, 14, 3013-3037, <https://doi.org/10.5194/essd-14-3013-2022>, 2022.
- Jin, Z., Wang, T., Zhang, H., Wang, Y., Ding, J., and Tian, X.: Constraint of satellite CO<sub>2</sub> retrieval on the global carbon cycle from a Chinese atmospheric inversion system, *SCIENCE CHINA Earth Sciences*, 66, <https://doi.org/10.1007/s11430-022-1036-7>, 2023.
- Kong, Y., Zheng, B., Zhang, Q., and He, K.: Global and regional carbon budget for 2015–2020 inferred from OCO-2 based on an ensemble Kalman filter coupled with GEOS-Chem, *Atmos. Chem. Phys.*, 22, 10769-10788, 10.5194/acp-22-10769-2022, 2022.
- Peiro, H., Crowell, S., Schuh, A., Baker, D. F., O'Dell, C., Jacobson, A. R., Chevallier, F., Liu, J., Eldering, A., Crisp, D., Deng, F., Weir, B., Basu, S., Johnson, M. S., Philip, S., and Baker, I.: Four years of global carbon cycle observed from the Orbiting Carbon Observatory 2 (OCO-2) version 9 and in situ data and comparison to OCO-2 version 7, *Atmos. Chem. Phys.*, 22, 1097-1130, 10.5194/acp-22-1097-2022, 2022.
- Peters, W., Jacobson, A. R., Sweeney, C., Andrews, A. E., Conway, T. J., Masarie, K., Miller, J. B., Bruhwiler, L. M. P., Petron, G., Hirsch, A. I., Worthy, D. E. J., van der Werf, G. R., Randerson, J. T., Wennberg, P. O., Krol, M. C., and Tans, P. P.: An atmospheric perspective on North American carbon dioxide exchange: CarbonTracker, *Proceedings of the National Academy of Sciences of the United States of America*, 104, 18925-18930, <https://doi.org/10.1073/pnas.0708986104>, 2007.
- Regnier, P., Resplandy, L., Najjar, R. G., and Ciais, P.: The land-to-ocean loops of the global carbon cycle, *Nature*, 603, 401-410, 10.1038/s41586-021-04339-9, 2022.
- Takahashi, T., Sutherland, S. C., Wanninkhof, R., Sweeney, C., Feely, R. A., Chipman, D. W., Hales, B., Friederich, G., Chavez, F., Sabine, C., Watson, A., Bakker, D. C. E., Schuster, U., Metzl, N., Yoshikawa-Inoue, H., Ishii, M., Midorikawa, T., Nojiri, Y., Koertzinger, A., Steinhoff, T., Hoppema, M., Olafsson, J., Arnarson, T. S., Tilbrook, B., Johannessen, T., Olsen, A., Bellerby, R., Wong, C. S., Delille, B., Bates, N. R., and de Baar, H. J. W.: Climatological mean and decadal change in surface ocean pCO<sub>2</sub>, and net sea-air CO<sub>2</sub> flux over the global oceans, *Deep-Sea Research Part II- Topical Studies in Oceanography*, 56, 554-577, <https://doi.org/10.1016/j.dsr2.2008.12.009>, 2009.
- Zhang, H., Tian, X., Cheng, W., and Jiang, L.: System of Multigrid Nonlinear Least-squares Four-dimensional Variational Data Assimilation for Numerical Weather Prediction (SNAP): System Formulation and Preliminary Evaluation, *Advances in Atmospheric Sciences*, 37, 1267-1284, 10.1007/s00376-020-9252-1, 2020.